JCTC Journal of Chemical Theory and Computation

pubs.acs.org/JCTC Article

Time-Dependent Second-Order Green's Function Theory for Neutral Excitations

Wenjie Dou,* Joonho Lee,* Jian Zhu,* Leopoldo Mejía,* David R. Reichman,* Roi Baer,* and Eran Rabani*

Cite This: https://doi.org/10.1021/acs.jctc.2c00057 Read Online

ACCESS | Metrics & More | Article Recommendations | Supporting Information

ABSTRACT: We develop a time-dependent second-order Green's function theory (GF2) for calculating neutral excited states in molecules. The equation of motion for the lesser Green's function (GF) is derived within the adiabatic approximation to the Kadanoff−Baym (KB) equation, using the second-order Born approximation for the self-energy. In the linear response regime, we recast the time-dependent KB equation into a Bethe−Salpeter-like equation (GF2-BSE), with a kernel approximated by the second-order Coulomb self-energy. We then apply our GF2-BSE to a set of molecules and atoms and find that GF2-BSE is superior to configuration interaction with singles (CIS) and/or time-dependent Hartree−Fock (TDHF), particularly for charge-transfer excitations, and is comparable to CIS with perturbative doubles (CIS(D)) in most cases.

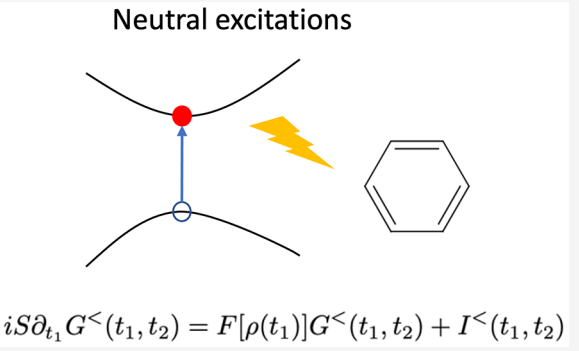

I. INTRODUCTION

Calculating excited states in molecules remains one of the grand challenges for computational chemistry. Time-dependent Hartree−Fock (HF)[1,2] and time-dependent density functional theory (DFT)[3−10] offer affordable and simple means to calculate excited-state energies, but suffer from accuracy with the corresponding excitation energies deviating by up to several electron volts. Other quantum chemistry methods, such as coupled cluster (CC) with singles and doubles within the equation-of-motion formalism (EOM-CCSD), are more accurate, but are limited to relatively small system sizes, because of the steep computational scaling.

An alternative to the above is based on many-body perturbation theory (MBPT) within Green's function theory. In particular, the so-called "GW" approximation and the Bethe−Salpeter equation (BSE) have been successful in predicting charge and optical excitation, respectively, particularly for solids.[11−26] However, the application of MBPT is often limited to simple solids with small unit cells, which has led to many efforts in recent years aiming to reduce the computational cost of MBPT-based techniques.[27−34]

The second-order Green's function (GF2) approach falls into this MBPT category. However, it has remained somewhat less popular than the GW/BSE approaches. Recently, GF2 theory has experienced a renaissance,[35−37] partially due to its simplicity and the inclusion of dynamical exchange effects. In GF2, the self-energy is described by the second-order Born approximation,[38,39] resulting in a class of dynamical exchange effects[40−42] that appear only at second and higher orders, and thus are often ignored in GW/BSE. On the other hand, GF2 treats the polarization term differently than GW/BSE and its accuracy in describing excited states in molecules is unexplored. The inclusion of such dynamical exchange terms in GF2 leads to $O(N^5)$ scaling of the computational cost where N is the size of the system.

To overcome this computational bottleneck of GF2, we have recently introduced a stochastic approach to GF2 (sGF2), based on a stochastic resolution of identity used to decouple the four-index Coulomb integrals.[43−45] Unlike the standard resolution of identity (RI),[46−50] the number of stochastic orbitals (playing the role of the resolution basis) does not increase with the system size for certain size-intensive ground-state properties,[44] as well as for quasiparticle excitations.[45] This allows one to reduce the computational scaling of sGF2 theory to $O(N^3)$ at the expense of introducing a controlled statistical error in the calculated observable. Similar stochastic approaches to electronic structure theory have been developed also for other frameworks, including GW,[29,51] DFT,[52−55] second-order Moller−Plesset (MP2),[43,56−58] and RPA,[59] and, more recently, they have also been used to improve the performance of auxiliary-field quantum Monte Carlo.[60]

Received: January 17, 2022
Revised: August 10, 2022
Accepted: August 12, 2022

In previous work, we have used the imaginary time and real-time sGF2 theory to calculate the ground-state and quasi-particle properties of molecular systems and assessed the accuracy of the stochastic resolution of identity for GF2.[44,45] Furthermore, we have introduced a range-separated stochastic RI approach, where the long-range Coulomb term was approximated by the stochastic RI and the short-range Coulomb term was described by a deterministic RI.[61] This hybrid deterministic-stochastic range-separated RI reduces the stochastic noise while maintaining the $O(N^3)$ computational scaling, which allows us to calculate the quasi-particle spectrum for systems containing $N = 1000$ electrons or more.[61]

In the present work, we extend the GF2 formalism to describe neutral excitations by considering explicitly the optical field within a time-dependent nonequilibrium GF2 theory. Unlike the equilibrium case, nonequilibrium Green's functions are dependent on two times and, thus, are more challenging to compute. Here, to simplify the calculation, we first invoke an adiabatic approximation to obtain the self-energy. We then derive within linear response theory a Bethe−Salpeter-like equation along with the second-order Born approximation to describe the Bethe−Salpeter kernel. While our long-term goal is to go beyond the adiabatic approximation and to develop a stochastic approach to reduce the scaling of the GF2 theory for excited states to $O(N^3)$, here, we focus on assessing the accuracy of GF2 for neutral excitations and comparing the approach to other methods, such as second-order approximation to EOM-CCSD (EOM-CC2) and configuration interaction with singles and perturbative doubles (CIS(D)). We note, in passing, that while it is difficult to formulate a stochastic version of EOM-CCSD with favorable scaling (as compared to the $O(N^3)$ of a stochastic GF2), some of us are formulating a stochastic version of EOM-CC2,[62] which will be comparable to GF2, in terms of scaling.

We show, at least in some simple but paradigmatic examples, that the time-dependent GF2 theory provides a more accurate framework to predict excited states compared to TDHF and configuration interaction with singles (CIS), and is competitive with and CIS(D) and EOM-CC2. In particular, for charge transfer states, CIS fails to predict the correct energy, whereas sGF2 provides a more reliable estimate of charge transfer excitations.

The manuscript is organized as follows: In Sections II and III, we present the formulation of the time-dependent GF2 theory in both the time and frequency domains. In Section IV, we test the performance of GF2 theory against other quantum chemistry methodologies for a representative set of atoms and molecules. Finally, in Section V, we present conclusions.

II. THEORY

II.A. Notation. We start by defining a general electronic Hamiltonian in second quantization form. The formulation is general and applies to any choice of basis set. In this section, we us the notation $i, j, k, l, \ldots$ to represent the indices in a general basis. The Hamiltonian is given by

$$\hat{H} = \hat{H}_0 + \sum_{ij} \Delta_{ij}(t)\hat{a}_i^\dagger \hat{a}_j \tag{1}$$

where $\hat{a}_i^\dagger$ ($\hat{a}_i$) is the creation (annihilation) operator for an electron in orbital $\chi_i(\mathbf{r})$, $\hat{H}_0$ is the unperturbed Hamiltonian, which is defined as

$$\hat{H}_0 = \sum_{ij} h_{ij}\hat{a}_i^\dagger \hat{a}_j + \frac{1}{2}\sum_{ijkl} v_{ijkl}\hat{a}_i^\dagger \hat{a}_k^\dagger \hat{a}_l \hat{a}_j \tag{2}$$

h_{ij} is the one-body matrix element in the basis, and v_{ijkl} represents the two-body, four-index Coulomb integral, given by

$$v_{ijkl} = (ij|kl) = \iint \frac{\chi_i(\mathbf{r}_1)\chi_j(\mathbf{r}_1)\chi_k(\mathbf{r}_2)\chi_l(\mathbf{r}_2)}{|\mathbf{r}_1 - \mathbf{r}_2|}\, d\mathbf{r}_1\, d\mathbf{r}_2 \tag{3}$$

The last term on the right-hand side of eq 1 represents a time-dependent perturbation, which is assumed to be one-body, suitable for describing the linear absorption spectrum, where $\Delta_{ij}(t)$ is the time-dependent one-body matrix element of the perturbation. In situations where the chosen basis is not orthonormal, we also define the overlap S with the overlap matrix elements of orbital $\chi_i(\mathbf{r})$ and $\chi_j(\mathbf{r})$ as

$$S_{ij} = (i|j) = \int \chi_i(\mathbf{r})\chi_j(\mathbf{r})\, d\mathbf{r} \tag{4}$$

II.B. Green's Function and Kadanoff−Baym Equations. The traditional approach to describe excited states generated by the Hamiltonian (eq 1) is based on solving the many-body eigenvalue problem, $H|\Psi_n\rangle = E_n|\Psi_n\rangle$, where E_n and $|\Psi_n\rangle$ are the nth eigenvalue and eigenstate, respectively. A complete solution within full configuration-interaction (FCI) is prohibitive for large system sizes or large atomic basis sets, and thus, most excited state calculations are based on introducing approximations with reduced computational scaling.

The Green's function formalism offers a systematic way to treat the many-body interactions in eq 1 using diagrammatic expansions. A central quantity in this approach is the single particle lesser Green's function defined as

$$G_{ij}^<(t_1, t_2) = i\langle \hat{a}_j^\dagger(t_2)\hat{a}_i(t_1)\rangle \tag{5}$$

(we assume that $\hbar = 1$).

In the above, we have used the Heisenberg representation for the time-dependent operator

$$\hat{a}_j^\dagger(t) = \mathcal{T} e^{i\int_0^t \hat{H}(t')\, dt'} \hat{a}_j^\dagger e^{-i\int_0^t \hat{H}(t')\, dt'} \tag{6}$$

where $\mathcal{T}$ is the time-ordering operator and the expectation value is calculated within the Grand Canonical ensemble: $\langle\cdots\rangle = Z^{-1}\mathrm{Tr}[(\cdots)e^{-\beta(\hat{H}_0 - \mu\hat{N})}]$. Here, $Z = \mathrm{Tr}[e^{-\beta(\hat{H}_0 - \mu\hat{N})}]$ is the Grand Canonical partition function, β the inverse temperature, μ the chemical potential, and N the number operator ($\hat{N} = \sum_i \hat{a}_i^\dagger \hat{a}_i$).

The equations of motion for the lesser Green's function follow the Kadanoff−Baym equations:[38]

$$iS\partial_{t_1} G^<(t_1, t_2) = F[\rho(t_1)]G^<(t_1, t_2) + I^<(t_1, t_2) \tag{7}$$

and

$$-i\partial_{t_2} G^<(t_1, t_2)S = G^<(t_1, t_2)F[\rho(t_2)] - I^<(t_2, t_1)^* \tag{8}$$

where $\rho(t) = -iG^<(t, t)$ is the density matrix, and $F[\rho]$ is the Fock operator with matrix elements

$$F_{ij}[\rho] = h_{ij} + v_{ij}^H[\rho] + v_{ij}^x[\rho] + \Delta_{ij}(t) \tag{9}$$

In the above, $v_{ij}^H[\rho] = \sum_{kl} v_{ijkl}\rho_{kl}$ is the matrix element of the Hartree potential and $v_{ij}^x = \sum_{kl} v_{ikjl}\rho_{kl}$ is the matrix element of the exchange interaction. Finally, the scattering integral, $I^<(t_1, t_2)$, appearing in eqs 7 and 8 is given by

https://doi.org/10.1021/acs.jctc.2c00057
J. Chem. Theory Comput. XXXX, XXX, XXX−XXX

$$I^{<}(t_1, t_2) = \int_0^{t_1} \Sigma^R(t_1, t_3) G^{<}(t_3, t_2)\, dt_3 + \int_0^{t_2} \Sigma^{<}(t_1, t_3) G^A(t_3, t_2)\, dt_3 \tag{10}$$

In the above equation, $G^A(t_1, t_2) = i\theta(t_2 - t_1)\langle \hat{a}_j^\dagger(t_2)\hat{a}_i(t_1)\rangle$ is the advanced Green's function and $\theta(t)$ is the Heaviside step-function. The exact form of the retarded ($\Sigma^R(t_1, t_2)$) and lesser ($\Sigma^{<}(t_1, t_2)$) self-energies is difficult to obtain apart from the case of simple model systems and, thus, most GF calculations are based on approximating the self-energies using different closures.

II.C. Second-Order Born Approximation to the Self-Energy (GF2 Theory). In this work, we resort to the second-order Born approximation to compute the self-energies (i.e., GF2 theory) and, as will become clear below, we describe only the retarded self-energy appearing above (Langreth rules have been used[38])

$$\Sigma_{ij}^R(t_1, t_2) = \sum_{mn} iG_{mn}^{<}(t_1, t_2)\delta W_{imjn}^R(t_1, t_2) + iG_{mn}^R(t_1, t_2)\delta W_{imjn}^{>}(t_1, t_2) \tag{11}$$

where the retarded and greater screened Coulomb integrals are given by

$$\delta W_{imjn}^R(t_1, t_2) = -i\sum_{klqp} (G_{kl}^{<}(t_1, t_2)G_{qp}^A(t_2, t_1) + G_{kl}^R(t_1, t_2)G_{qp}^{<}(t_2, t_1))v_{impk}(2v_{jnql} - v_{jlqn}) \tag{12}$$

$$\delta W_{imjn}^{>}(t_1, t_2) = -i\sum_{klqp} G_{kl}^{>}(t_1, t_2)G_{qp}^{<}(t_2, t_1)v_{impk}(2v_{jnql} - v_{jlqn}) \tag{13}$$

and, as before, $G_{ij}^{R,A}(t_1, t_2)$ and $G_{ij}^{<,>}(t_1, t_2)$ are the retarded/advanced and the lesser/greater Green's function, respectively.

II.D. The Adiabatic Approximation. Before we proceed, we would like to point out to another challenge associated with the need to propagate the GF and to evaluate the self-energies along two times. In the following subsection, we will invoke the adiabatic approximation similarly to the approach taken for GW/BSE.[63] This allows us to reduce the complexity associated with describing two-time self-energies. The idea behind the adiabatic approximation is that the system responds instantaneously to the external driving force such that the integral in eq 10 becomes local in time.

It is convenient to define the central time t and the time difference τ:

$$t = \frac{(t_1 + t_2)}{2} \tag{14}$$

$$\tau = t_1 - t_2 \tag{15}$$

and express the self-energies appearing in the scattering integral (cf., eq 10) by[63]

$$\Sigma^R(t_1, t_2) \approx \tilde{\Sigma}^{ad}(t)\delta(\tau) \tag{16}$$

$$\Sigma^{<}(t_1, t_2) \approx 0 \tag{17}$$

In the above equation, $\tilde{\Sigma}^{ad}(t)$ is defined as

$$\tilde{\Sigma}^{ad}(t) = \int \Sigma^R(t_1, t_2)e^{i\omega\tau}\, d\tau \equiv \tilde{\Sigma}^R(t, \omega) \tag{18}$$

The adiabatic approximation is consistent with taking the $\omega \to 0$ limit assuming that the plasma energy (the main source of screening) is much higher than the neutral excitation energy differences.[64] Note that, in the above equation, $\tilde{\Sigma}^{ad}(t)$ is given in terms of a Fourier transform of the time difference variable, τ denoted by a "tilde" ($\tilde{\cdot}$).

Using the adiabatic approximation for the self-energy, the equation of motion for the equal time Green's function, $-iG^{<}(t_1 = t, t_2 = t) = \rho(t)$, can be simplified as

$$i\partial_t\rho(t) = S^{-1}(F[\rho(t)] + \tilde{\Sigma}^{ad}(t))\rho(t) - \rho(t)(F[\rho(t)] + \tilde{\Sigma}^{ad\dagger}(t))S^{-1} \tag{19}$$

where $\rho(t)$ is the density matrix and $\tilde{\Sigma}^{ad}(t)$ is defined in eq 18. In principle, the solution of the above equation requires a knowledge of the retarded and lesser Green's functions as well as the screened Coulomb kernel to obtain $\tilde{\Sigma}^{ad}(t)$ from eq 18. While this seems challenging, the adiabatic limit offers a significant simplification within the weak perturbation limit, as described in the following section.

III. THE WEAK DRIVING LIMIT

In the limit of weak external perturbation, namely, when $\Delta_{ij}(t) \to 0$, we can further simplify the description of the self-energy and recast the time-dependent equation of motion for the density matrix into a Casida-like form. In this section, we first provide a working expression to obtain the $\tilde{\Sigma}^{ad}(t)$ without solving the Kadanoff−Baym equations for the retarded and lesser Green's functions, and then derive a Casida-like equation to describe the neutral (excitonic) spectrum within the GF2 closure.

III.A. Self-Energy. So far, the formalism described above makes no assumption about the basis set used. However, using the eigenvalues of eq 9 with $\Delta_{ij}(t) = 0$ leads to a significant simplification. Thus, we now describe the calculation of $\Sigma^{ad}(t)$ using the eigenstates (ψ_i) and the eigenvalues (ε_i) of the Fock matrix. To obtain an expression for $\Sigma^{ad}(t)$, we treat the two terms appearing on the right-hand side of eq 11 separately, and refer to the corresponding self-energies with superscripts "ad1" and "ad2". For $\tilde{\Sigma}_{ij}^{ad1}(t)$, we further use an approximation[63,64] for the lesser Green's function given by $G_{ij}^{<}(t, \omega) = i2\pi\delta(\omega - \varepsilon_i)G_{ij}^{<}(t, \tau = 0)$. This leads to the following expression for $\tilde{\Sigma}_{ij}^{ad1}(t)$ (see Appendix A for more details)

$$\tilde{\Sigma}_{ij}^{ad1}(t) \approx i\sum_{mn} \delta\tilde{W}_{imjn}^R(-\epsilon_m)G_{mn}^{<}(t, \tau = 0) = -\sum_{kl} \delta\tilde{W}_{imjn}^R(-\epsilon_m)\rho_{mn}(t) \tag{20}$$

where, as before, $\rho_{kl}(t)$ is the kl matrix element of the density matrix. Following similar steps for $\tilde{\Sigma}_{ij}^{ad2}(t)$ we obtain (see Appendix A for more details)

$$\tilde{\Sigma}_{ij}^{ad2}(t) \approx \frac{1}{2}\Re\sum_{mn} \delta\tilde{W}_{imjn}^R(0)\delta_{mn} \tag{21}$$

https://doi.org/10.1021/acs.jctc.2c00057
J. Chem. Theory Comput. XXXX, XXX, XXX−XXX

Table 1. Difference of the Lowest Singlets (in eV) for CIS, TDHF, CIS(D), EOM-CC2, GW-BSE, G0F2-BSE, and EOM-CCSD against EOM-CC(2,3)

atom	state	ΔCIS (eV)	ΔTDHF (eV)	ΔCIS(D) (eV)	ΔEOM-CC2 (eV)	ΔEOM-CCSD (eV)	ΔG0W0-BSE (eV)	ΔG0F2-BSE (eV)	EOM-CC(2,3) (eV)
He	A_g	−0.72	−1.09	−0.11	−0.11	0.00	0.30	−0.05	52.66
	B_{2u}	−0.82	−0.98	−0.15	−0.15	0.00	0.27	−0.67	78.20
	B_{3u}	−0.82	−0.98	−0.15	−0.15	0.00	0.27	−0.67	78.20
	B_{1u}	−0.82	−0.98	−0.15	−0.15	0.00	0.27	−0.67	78.20
error		0.79	1.01	0.14	0.14	0.00	0.28	0.51	0
Be	B_{2u}	−0.33	−0.63	−0.18	−0.19	0.00	−0.17	−0.17	5.63
	B_{3u}	−0.33	−0.63	−0.18	−0.19	0.00	−0.17	−0.17	5.63
	B_{1u}	−0.33	−0.63	−0.18	−0.19	0.00	−0.17	−0.17	5.63
error		0.33	0.63	0.18	0.19	0.00	0.17	0.17	0
Ne	$1B_{1g}$	−1.01	−1.15	0.17	0.21	0.04	−0.07	0.82	50.02
	$1B_{2g}$	−1.01	−1.15	0.17	0.21	0.04	−0.07	0.82	50.02
	$1B_{3g}$	−1.01	−1.15	0.17	0.21	0.04	−0.07	0.82	50.02
	$1A_g$	−1.05	−1.12	0.18	0.21	0.04	0.01	0.73	50.52
	$2A_g$	−1.05	−1.12	0.18	0.21	0.04	0.01	0.73	50.52
error		1.03	1.14	0.18	0.21	0.04	0.04	0.79	0

Note that $\tilde{\Sigma}^{ad2}_{ij}(t)$ is time-independent. Using the zeroth order approximation to the Green's functions appearing in eq 12, we find that

$$\begin{aligned}\delta\tilde{W}^{R}_{imjn}(\omega) = &\sum_{klpq}\left[f(\epsilon_l)\frac{1}{\epsilon_l-\omega-\epsilon_q-i\eta}\right.\\ &\left.+\frac{1}{\omega+\epsilon_p-\epsilon_l+i\eta}f(\epsilon_p)\right]\\ &\times\delta_{kl}\delta_{pq}v_{impk}(2v_{jnql}-v_{jlqn})\\ =&\sum_{kq}\frac{f(\epsilon_k)-f(\epsilon_q)}{\epsilon_k-\omega-\epsilon_q-i\eta}v_{imqk}(2v_{jnqk}-v_{jkqn})\end{aligned} \tag{22}$$

In the above equation, η is a small positive regularization parameter, and $f(\varepsilon_n)$ is the Fermi−Dirac distribution.

III.B. Linear Response Theory: GF2-BSE. For reasons that will become clear below, we denote the initial density matrix $\rho(t=0) \equiv \rho_0$ and the initial self-energy as $\Sigma^{ad}(0) \equiv \Delta H$. Furthermore, we reorganize eq 19 into a more suitable form for introducing the Bethe−Salpeter equation:

$$\begin{aligned}i\partial_t\rho = &S^{-1}(F[\rho_0]+\Delta H+v^H[\rho]-v^H[\rho_0]+v^x[\rho]-v^x[\rho_0])\rho\\ &-\rho(F[\rho_0]+\Delta H+v^H[\rho]-v^H[\rho_0]+v^x[\rho]-v^x[\rho_0])S^{-1}\\ &+S^{-1}(\Sigma^{ad}(t)-\Sigma^{ad}(t=0))\rho-\rho(\Sigma^{ad\dagger}(t)-\Sigma^{ad\dagger}(t=0))S^{-1}\end{aligned} \tag{23}$$

In the applications reported below, we obtain the quasiparticle-like correction term (ΔH) from a stochastic GF2 calculation[45] and the adiabatic self-energy ($\Sigma^{ad}(t)$) using the second-order Born approximation. The above equation can be used to describe both weak and strong driving forces, $\Delta(t)$ but can be further simplified into a Casida-like form within linear response theory (assuming weak driving forces).

Following the general guidelines used in time dependent DFT or TDHF,[4,10,63] the time-dependent GF2 can be recast into a symplectic eigenvalue problem (assuming zero temperature and spin-restricted orbitals)

$$\begin{pmatrix}A & B\\ -B & -A\end{pmatrix}\begin{pmatrix}X\\ Y\end{pmatrix}=\omega\begin{pmatrix}X\\ Y\end{pmatrix} \tag{24}$$

where A and B are matrices of size $N_{occ}N_{virt}\times N_{occ}N_{virt}$ and N_{occ}/N_{virt} is the number of occupied/virtual molecular orbitals. These matrices can be expressed in terms of the exchange K^X and direct K^{DA} correlations

$$\begin{aligned}A &= D+2K^X-K^{DA}\\ B &= 2K^X-K^{DB}\end{aligned} \tag{25}$$

The matrix elements of D, K^X, and K^{DA} are given by

$$\begin{aligned}D_{ia,jb} &= (\omega_a-\omega_i)\delta_{ab}\delta_{ij}\\ K^X_{ia,jb} &= \iint d\mathbf{r}_1\, d\mathbf{r}_2\frac{(\psi_i(\mathbf{r}_1))^*\psi_a(\mathbf{r}_1)(\psi_j(\mathbf{r}_2))^*\psi_b(\mathbf{r}_2)}{|\mathbf{r}_1-\mathbf{r}_2|}\\ K^{DA}_{ia,jb} &= \delta\tilde{W}^R_{abij}+v_{abij}\\ K^{DB}_{ia,jb} &= \delta\tilde{W}^R_{ibaj}+v_{ibaj}\end{aligned} \tag{26}$$

Here, i, j represents occupied orbitals and a, b are unoccupied orbitals. $\omega_{a,i}$ is the GF2-corrected quasiparticle energy in the molecular basis obtained by solving for[45]

$$\omega_n = \varepsilon_n+\langle\psi_n|\Re\tilde{\Sigma}^R(\omega_n)|\psi_n\rangle \tag{27}$$

where $\Sigma^R(\omega_n)$ is the self-energy obtained from a single-time GF2 calculation.[45] eqs 24−26 are the main result of this subsection and are referred to as "GF2-BSE".

III.C. Computational Scaling and Outline of the Approach. The overall computational scaling of solving eq 23 for $\rho(t)$ is determined by the computational scaling of the self-energy, which is the most expansive part of the calculation. Formally, the scaling of the self-energy is $O(N^5)$, where N is the size of the basis. In linear response, the computational scaling for the GF2-BSE is $O(n_{root}N^5)$ with n_{root} being the number of roots, a common increase in scaling going from the time domain to the frequency domain.[4,63] A significant reduction in the overall scaling to cubic ($O(n_{root}N^3)$) can be achieved using a stochastic resolution of identity,[43,44] applied to the time-domain

https://doi.org/10.1021/acs.jctc.2c00057
J. Chem. Theory Comput. XXXX, XXX, XXX−XXX

Table 2. Difference of the Several Lowest Vertical Excitation Energies for H_2 Using CIS, TDHF, CIS(D), EOM-CC2, GW-BSE, G0F2-BSE, EOM-CCSD against EOM-CC(2,3) Approach

H_2	state	ΔCIS (eV)	Δ*T*DHF (eV)	ΔCIS(D) (eV)	Δ*E*OM-CC2 (eV)	ΔG0W0-BSE (eV)	ΔG0F2-BSE (eV)	EOM-CCSD (eV)	EOM-CC(2,3) (eV)
	$1B_{1u}$	0.15	−0.01	0.11	0.10	0.22	−0.14	0.00	13.91
	$1A_g$	0.06	−0.08	0.18	0.16	0.55	−0.22	0.00	21.40
	$2B_{1u}$	1.29	1.04	0.94	0.97	1.10	0.89	0.00	30.98
	$1B_{2u}$	−0.27	−0.41	0.03	0.03	0.38	−0.65	0.00	40.57
	$1B_{3u}$	−0.27	−0.41	0.03	0.03	0.38	−0.65	0.00	40.57
error		0.41	0.39	0.26	0.26	0.53	0.51	0.00	0

Table 3. Difference of the Lowest Singlet Energy () from CIS, TDHF, CIS(D), EOM-CC2, GF2-BSE, EOM-CCSD against EOM-CC(2,3) for a List of Molecules[a]

	state	ΔCIS (eV)	Δ*T*DHF (eV)	ΔCIS(D) (eV)	ΔEOM-CC2 (eV)	ΔEOM-CCSD (eV)	ΔG0W0-BSE (eV)	ΔGF2-BSE (eV)	EOM-CC(2,3) (eV)
LiH	$1A_1$	0.58	0.54	0.25	0.26	0.00	0.24	0.04 ± 0.11	3.47
	$1B_1$	0.60	0.58	0.26	0.26	0.00	0.32	0.09 ± 0.12	4.49
	$1B_2$	0.60	0.58	0.26	0.26	0.00	0.32	0.12 ± 0.12	4.49
	$2A_1$	0.45	0.39	0.26	0.26	0.00	0.31	0.15 ± 0.11	6.49
	$2B_1$	0.49	0.48	0.25	0.25	0.00	0.13	−0.15 ± 0.12	7.37
	$2B_2$	0.49	0.48	0.25	0.25	0.00	0.13	−0.12 ± 0.13	7.37
error		0.54	0.51	0.25	0.26	0.00	0.24	0.11 ± 0.12	0
LiF	$1B_1$	1.79	1.78	−1.46	−0.97	−0.05	−0.23	−0.42 ± 0.50	6.09
		(−0.02)	(−0.01)		(−0.52)	(4.72)	(0.07)	(0.11 ± 0.01)	
	$1B_2$	1.79	1.78	−1.46	−0.97	−0.05	−0.23	−0.29 ± 0.50	6.09
	$1A_1$	2.03	2.02	−1.64	−1.13	−0.03	−0.15	−0.60 ± 0.55	6.47
	$1A_2$	1.50	1.46	−1.13	−0.84	−0.06	−0.22	−0.13 ± 0.48	7.79
	$2A_1$	1.52	1.50	−1.20	−0.84	−0.06	−0.21	−0.06 ± 0.47	7.79
	$2A_2$	1.48	1.45	−1.25	−0.84	−0.07	−0.25	−0.04 ± 0.46	7.83
error		1.68	1.67	1.36	0.93	0.05	0.22	0.26 ± 0.50	0
H_2O	$1B_2$	0.95	0.90	−0.18	−0.16	−0.08	0.21	−0.27 ± 0.35	8.27
		(1.07)	(1.13)		(−0.78)	(8.17)	(0.22)	(−0.35 ± 0.03)	
	$1A_2$	0.70	0.63	−0.11	−0.14	−0.06	0.23	−0.02 ± 0.38	10.30
	$1A_1$	0.94	0.88	−0.17	−0.15	−0.06	0.22	−0.28 ± 0.42	10.89
	$1B_1$	0.66	0.56	−0.10	−0.12	−0.05	0.21	−0.12 ± 0.40	12.97
	$2B_1$	0.19	0.14	−0.06	−0.04	−0.01	0.11	−0.60 ± 0.54	14.89
	$2A_1$	0.43	0.21	−0.09	−0.08	0.01	0.12	−0.54 ± 0.56	17.95
error		0.64	0.55	0.12	0.11	0.05	0.18	0.30 ± 0.44	0

[a]Numbers in parentheses indicate the binding energy for EOM-CCSD and errors in the binding energy, with respect to that of EOM-CCSD for other methods.

formulation, which will be the subject of future study. Here, we focus on assessing the accuracy of the GF2-BSE approach to describe neutral excisions. Before doing so, we outline the main steps for such calculation:

(1) Perform a Hartree−Fock calculation and generate the Fock matrix (eq 9).
(2) Use the single-time GF2 approach[45] to calculate the self-energy appearing in eq 27 and obtain the GF2 correction to the quasi-particle energies, ω_n.
(3) Calculate $\delta\tilde{W}^R_{im,jn}(\omega = 0)$ using eq 22. For the applications reported below, we used a damping parameter (η = 0.01 au), which is sufficiently small to converge the results.
(4) Calculate the matrix elements of eq 24, and solve for the eigenvalues and eigenstates.

Solving for ω_n is done self-consistently both for solving eq 27 and also for obtaining $\tilde{\Sigma}^R(\omega)$. A simplification that often is useful within the framework of GW/BSE is to use a single-shot calculation, which amounts to replacing $\tilde{\Sigma}^R(\omega)$ with the zeroth order approximation.[64] However, this may result in multiple solutions for ω_n and, in such cases, we restrict the solution to the fully self-consistent treatment.[45] We denote the former approach as G0F2-BSE and the latter as GF2-BSE.

IV. APPLICATIONS TO ATOMS AND MOLECULES

In this section, we compare results obtained using the GF2-BSE approach for the low-lying excited states for a set of atoms and molecules, and compare GF2-BSE results to results obtained using CIS, TDHF, CIS(D), GW-BSE, EOM-CCSD, EOM-CC2, and EOM-CC(2,3) methods. The latter (EOM-CC(2,3)) is the most accurate among the methods compared here, and is used as our references. We use the cc-pVDZ basis set for most cases discussed below, unless otherwise noted.

In Table 1, we list several lowest singlet excited-state energy differences (compared to the corresponding EOM-CC(2,3) singlet energies) for several closed-shell atoms. The bottom row

https://doi.org/10.1021/acs.jctc.2c00057
J. Chem. Theory Comput. XXXX, XXX, XXX−XXX

Table 4. Difference of the Lowest Singlet Energy (in eV) from CIS, TDHF, CIS(D), EOM-CC2, and GF2-BSE against EOM-CCSD for the Listed Molecules[a]

	state	ΔCIS (eV)	Δ*T*DHF (eV)	ΔCIS(D) (eV)	Δ*E*OM-CC2 (eV)	ΔG0W0-BSE (eV)	ΔGF2-BSE (eV)	EOM-CCSD (eV)
NH_3	A′	0.90	0.86	0.02	0.01	0.31	0.65 ± 0.49	7.59
		(0.87)	(0.91)		(−0.66)	(0.23)	(−0.27 ± 0.01)	(7.13)
	A′′	0.58	0.51	0.04	0.00	0.31	0.82 ± 0.50	9.85
	A′	0.58	0.51	0.04	0.00	0.31	0.94 ± 0.48	9.85
	A′′	0.34	0.31	0.04	0.02	0.21	0.36 ± 0.36	13.38
	A′	0.34	0.31	0.04	0.02	0.21	0.50 ± 0.35	13.38
	A′′	0.40	0.35	0.06	0.05	0.26	0.57 ± 0.35	15.55
	A′′	0.34	0.30	0.01	0.03	0.24	0.58 ± 0.35	15.71
	A′	0.34	0.30	0.01	0.03	0.24	0.65 ± 0.35	15.71
error		0.48	0.43	0.03	0.02	0.26	0.63 ± 0.40	0
HCN	A_2	−1.49	−1.99	0.13	0.15	−0.43	−0.02 ± 0.35	8.81
		(1.83)	(2.33)		(−0.54)	(0.36)	(−0.74 ± 0.29)	(9.18)
	A_2	−1.41	−1.65	0.20	0.22	−0.30	0.04 ± 0.38	9.21
	A_1	−1.41	−1.65	0.20	0.22	−0.30	0.16 ± 0.42	9.21
	B_2	0.71	0.50	0.21	0.11	0.39	−0.15 ± 0.40	9.70
	B_1	0.71	0.50	0.21	0.11	0.39	0.05 ± 0.54	9.70
	B_1	0.37	0.33	0.10	0.12	0.08	−1.30 ± 0.56	11.29
	B_2	0.37	0.33	0.10	0.12	0.08	−0.82 ± 0.46	11.29
	A_1	2.20	1.27	0.67	−0.74	0.56	−1.17 ± 0.45	11.76
error		1.08	1.03	0.23	0.22	0.31	0.46 ± 0.45	0

[a]Numbers in parentheses indicate the binding energy for EOM-CCSD and errors in the binding energy, with respect to that of EOM-CCSD for other methods.

Table 5. Difference of the Lowest Singlet Energy (in eV) from CIS, TDHF, CIS(D), EOM-CC2, and GF2-BSE against EOM-CCSD for the Listed Molecules[a]

	state	ΔCIS (eV)	Δ*T*DHF (eV)	ΔCIS(D) (eV)	Δ*E*OM-CC2 (eV)	ΔG0W0-BSE (eV)	ΔGF2-BSE (eV)	EOM-CCSD (eV)
N_2	$1B_{3g}$	0.40 (fourth)	0.15 (fourth)	0.25	0.05	0.36 (second)	−0.13 ± 0.58	9.62
		(2.10)	(2.35)		(−0.85)	(0.25)	(−0.37 ± 0.34)	(9.70)
	$1B_{2g}$	0.40 (fourth)	0.15 (fourth)	0.25	0.05	0.36 (second)	0 ± 0.62	9.62
	$1A_u$	−1.83 (first)	−2.40 (first)	0.20	0.21	−0.57 (first)	0.17 ± 0.66	10.40
	$1B_{1u}$	−1.68 (second)	−1.96 (second)	0.32	0.34	−0.35	0.29 ± 0.66	10.83
	$2A_u$	−1.68 (second)	−1.96 (second)	0.32	0.34	−0.35	0.32 ± 0.66	10.83
	$1B_{2u}$	2.12	1.79	0.59	0.53	1.06	−0.3 ± 0.55	13.97
	$1B_{3u}$	2.12	1.79	0.59	0.53	1.06	−0.18 ± 0.59	13.97
	$2B_{1u}$	0.18	−1.46	0.08	−0.07	−1.19	−0.75 ± 0.74	17.00
error		1.30	1.46	0.33	0.27	0.66	0.27 ± 0.63	0
CO	$1B_1$	−0.05 (second)	−0.40 (second)	0.12 (second)	0.09	0.08 (fourth)	−1.32 ± 0.66	7.41
		(1.69)	(2.04)		(−0.63)	(0.90)	(−0.28 ± 0.15)	(8.78)
	$1B_2$	−0.05 (second)	−0.40 (second)	0.12 (second)	0.09	0.08 (fourth)	−1.13 ± 0.72	7.41
	$1A_2$	−0.53 (first)	−1.06 (first)	0.01 (first)	0.53	−0.53 (second)	−0.38 ± 0.89	7.48
	$1A_1$	−0.19	−0.46	0.16	0.75	−0.87 (third)	−0.05 ± 0.93	7.60
	$2A_2$	−0.19	−0.46	0.16	0.75	−1.36 (first)	−0.01 ± 0.93	7.60
	$2A_1$	0.96	−0.03	−1.00	−0.56	−0.08	−0.81 ± 0.99	11.86
	$2B_2$	1.96	1.67	0.52	0.52	0.26	−0.73 ± 0.75	12.59
	$2B_1$	1.96	1.67	0.52	0.52	0.26	−0.55 ± 0.77	12.59
error		0.73	0.77	0.33	0.48	0.44	0.62 ± 0.83	0

[a]Numbers in parentheses indicate the binding energy for EOM-CCSD and errors in the binding energy with respect to that of EOM-CCSD for other methods. 1st, 2nd, etc. are used to indicate the changes of the ordering of state as compared to the EOM-CCSD ordering (see main text for more details).

indicates the averaged absolute error. We find that the smallest deviations are observed for the CIS(D) approach, with an overall average error of ∼0.15 eV. The EOM-CC2 results are very similar to CIS(D) results, which is not too surprising given that both methods include electron correlation only up to second order. CIS and TDHF underestimate the excitation energies by an average of nearly 1 eV, while the G0F2-BSE approach outperforms CIS and TDHF with an average error of 0.5 eV; however, G0F2-BSE performs much better for the lowest singlet excitation. The G0F2-BSE underestimates the excitation energies in some cases, and in others, it overestimates them. The overall better performance of G0F2-BSE, with respect to

https://doi.org/10.1021/acs.jctc.2c00057
J. Chem. Theory Comput. XXXX, XXX, XXX−XXX

Table 6. Difference of the Lowest Singlet Energy from CIS, TDHF, CIS(D), EOM-CC2, and GF2-BSE against EOM-CCSD for the Listed Molecules[a]

	state	ΔCIS (eV)	ΔTDHF (eV)	ΔCIS(D) (eV)	ΔEOM-CC2 (eV)	ΔG0W0-BSE (eV)	ΔGF2-BSE (eV)	EOM-CCSD (eV)
CH_4	1A′	0.44	0.41	0.12	0.08	0.28	0.08 ± 0.47	12.31
		(0.80)	(0.82)		(−0.46)	(0.16)	(−0.22 ± 0.02)	(6.50)
	1A″	0.44	0.41	0.12	0.08	0.28	0.20 ± 0.48	12.31
	2A′	0.44	0.41	0.12	0.08	0.28	0.33 ± 0.47	12.31
	2A″	0.53	0.51	0.15	0.14	0.37	0.33 ± 0.47	14.03
	3A′	0.53	0.51	0.15	0.14	0.37	0.37 ± 0.48	14.03
	3A″	0.53	0.51	0.15	0.14	0.37	0.46 ± 0.48	14.03
	4A′	0.52	0.50	0.12	0.11	0.32	0.25 ± 0.48	14.32
	4A″	0.52	0.50	0.12	0.11	0.32	0.35 ± 0.48	14.32
error		0.50	0.47	0.13	0.11	0.32	0.30 ± 0.48	0
C_2H_6	$1A_g$	0.58	0.56	0.07	0.00	0.35	−0.38 ± 0.26	10.88
		(0.86)	(0.87)		(−0.43)	(0.19)	(−0.11 ± 0.26)	(5.95)
	$1B_g$	0.58	0.56	0.07	0.00	0.35	−0.20 ± 0.27	10.88
	$2A_g$	0.91	0.86	−0.02	−0.02	0.34	−0.10 ± 0.38	11.57
	$1B_u$	0.45	0.41	0.10	0.02	0.34	−0.29 ± 0.23	12.34
	$1A_u$	0.45	0.41	0.10	0.02	0.34	−0.10 ± 0.24	12.34
	$2A_u$	0.73	0.71	0.10	0.07	0.42	−0.14 ± 0.26	12.70
	$2B_u$	0.73	0.70	0.05	0.03	0.36	−0.23 ± 0.24	12.89
	$3A_u$	0.73	0.70	0.05	0.03	0.36	−0.13 ± 0.24	12.89
error		0.65	0.62	0.07	0.03	0.36	0.20 ± 0.27	0
C_3H_8	1A′	0.68	0.66	0.05	−0.03	0.40	−0.48 ± 0.43	10.48
	1A″	0.92 (third)	0.89 (third)	0.02	−0.08	0.39	−0.48 ± 0.47	10.71
	2A′	0.83 (second)	0.80 (second)	0.03	−0.06	0.39	−0.23 ± 0.52	10.79
	2A″	0.52	0.50	0.09	0.01	0.34	−0.41 ± 0.52	11.61
	3A″	0.64	0.62	0.00	−0.02	0.35	−0.36 ± 0.45	11.86
	4A″	0.87 (eighth)	0.85 (eighth)	0.00	−0.05 (seventh)	0.45 (eighth)	−0.39 ± 0.45	12.04
	3A′	0.81	0.78	0.03	−0.07 (sixth)	0.39 (sixth)	−0.29 ± 0.42	12.05
	4A′	0.62 (sixth)	0.57 (sixth)	0.09	−0.02	0.38 (seventh)	−0.25 ± 0.40	12.09
error		0.74	0.71	0.04	0.04	0.39	0.34 ± 0.46	0

[a]Numbers in parentheses indicate the binding energy for EOM-CCSD and errors in the binding energy with respect to that of EOM-CCSD for other methods. 1st, 2nd, etc. are used to indicate the changes of the ordering of state as compared to the EOM-CCSD ordering (see main text for more details).

CIS/TDHF results from two main attributes: (a) the inclusion of screening effects in the G0F2-BSE kernel (missing from both CIS and TDHF), which reduces the coupling between electrons and holes and (b) the correction of the quasi-particle energies, ω_n, that are assumed to equal the HF orbital energies in CIS/TDHF and thus overestimate the fundamental band gap (HOMO−LUMO gap). The error cancellation between the larger HF fundamental gap and the stronger Coulomb interactions give rise to an overall reasonable excitation energies using CIS and TDHF.

In Table 2, we list the lowest singlet excited-state energy differences (compared to the EOM-CC(2,3)) for the vertical excitation of H_2 molecule within the cc-pVDZ basis. Since there are only two electrons involved, the EOM-CCSD provides an exact solution for the basis set used. We excluded excited states with double excitation character since these states are not well-described by several methods, including CIS, TDHF, and the adiabatic approximation to GF2. We find that all methods provide similar accuracy of the excited states, compared to the EOM-CCSD across all excitation energies.

In Table 3, we list the vertical excitation energies for three different molecules obtained using the aforementioned methods. To reduce the scaling and the computational effort, we use the stochastic GF2 methods[45] to calculate the self-energies appearing in eq 27, as well as to obtain the GF2 correction (ΔH) to the quasi-particle energies, ω_n. Thus, the vertical excitation energies obtained from the GF2-BSE method have an error bar resulting for the use of a stochastic approach. We have used 2000 stochastic orbitals to obtain the full self-consistent self-energy. The stochastic errors from GF2-BSE are estimated using 10 independent runs. Note that here we have only used the stochastic formulation of Matsubara and mixed time GF2 to obtain the self-energy and hence quasi-particle energies. A full stochastic implementation of the GF2-BSE theory will be presented and tested in future work.

We first examine the vertical excitations LiH, LiF, and H_2O, as shown in Table 3. We find that for the entire range of excitations, the GF2-BSE approach outperforms CIS and TDHF, with an overall error that is smaller by a factor of 3, compared to the other two methods. Comparing the results obtained by the GF2-BSE with the CIS(D) and EOM-CC2, we find that, for the lower excitation energies, the two GF-based approach provide similar accuracies, while the CIS(D) and EOM-CC2 provide a better description of higher vertical excitations. For LiF, we find that CIS(D) and EOM-CC2 are rather poor, compared to the GF2-BSE (showing similar results to G0W0-BSE). LiF excited states have significant charge transfer character, which requires orbital

https://doi.org/10.1021/acs.jctc.2c00057
J. Chem. Theory Comput. XXXX, XXX, XXX−XXX

Table 7. Difference of the Lowest Singlet Energy from CIS, TDHF, CIS(D), EOM-CC2, GW-BSE, and GF2-BSE against EOM-CCSD for Hydrogen Fluoride (HF)

	state	ΔCIS (eV)	Δ*T*DHF (eV)	ΔCIS(D) (eV)	Δ*E*OM-CC2 (eV)	ΔG0W0-BSE (eV)	ΔGF2-BSE (eV)	EOM-CCSD (eV)
cc-pVDZ	$1B_2$	1.23	1.16	−0.20	−0.14	0.24	−0.31 ± 0.52	10.72
		(0.97)	(1.04)		(−0.77)	(0.15)	(−0.28 ± 0.01)	9.20
	$1B_1$	1.23	1.16	−0.20	−0.14	0.24	−0.15 ± 0.46	10.72
	$1A_1$	0.83	0.68	−0.17	−0.12	0.15	−0.32 ± 0.33	15.61
	$2B_1$	1.67	1.60	−0.15	0.04	−0.01	−0.80 ± 0.49	24.74
	$2B_2$	1.67	1.60	−0.15	0.04	−0.01	−0.63 ± 0.44	24.74
	$2A_1$	1.20	1.00	0.21	0.20	0.17	−0.21 ± 0.36	30.59
	$3A_1$	4.08	3.79	0.51	0.89	1.22	0.75 ± 0.62	34.29
	$2A_1$	−0.82	−0.75	0.28	0.20	−0.16	1.59 ± 0.60	39.03
error		1.59	1.47	0.23	0.22	0.28	0.60 ± 0.48	0
cc-pVTZ	$1B_2$	1.19	1.12	−0.33	−0.26	0.33	0.59 ± 0.50	10.77
		(0.89)	(0.96)		(−0.87)	(0.08)	(−0.30 ± 0.01)	(8.54)
	$1B_1$	1.19	1.12	−0.33	−0.26	0.33	0.75 ± 0.50	10.77
	$1A_1$	0.80	0.69	−0.25	−0.21	0.24	0.56 ± 0.46	15.31
	$2B_1$	1.44	1.37	−0.35	−0.16	0.07	0.32 ± 0.48	20.08
	$2B_2$	1.44	1.37	−0.35	−0.16	0.07	0.49 ± 0.47	20.08
	$2A_1$	0.91	0.81	−0.03	−0.01	0.12	0.57 ± 0.44	24.96
	$1A_2$	0.62	0.50	0.24	0.01	0.06	0.52 ± 0.58	27.02
	$3B_1$	0.73	0.68	−0.09	0.00	0.21	0.60 ± 0.59	27.09
error		1.04	0.96	0.25	0.13	0.18	0.55 ± 0.50	0
cc-pVQZ	$1B_2$	1.16	1.09	−0.40	−0.34	0.42	0.75 ± 0.54	10.76
		(0.81)	(0.88)		(−0.89)	(0.03)	(−0.31 ± 0.01)	(8.09)
	$1B_1$	1.16	1.09	−0.40	−0.34	0.42	0.93 ± 0.55	10.76
	$1A_1$	0.75	0.67	−0.30	−0.27	0.31	0.74 ± 0.53	15.15
	$2B_1$	1.24	1.17	−0.39	−0.26	0.17	0.65 ± 0.50	18.46
	$2B_2$	1.24	1.17	−0.39	−0.26	0.17	0.83 ± 0.51	18.46
	$3B_1$	1.02	0.99	−0.34	−0.17	0.29	1.33 ± 0.58	21.80
	$3B_2$	1.02	0.99	−0.34	−0.17	0.29	1.43 ± 0.56	21.80
	$1A_2$	0.71	0.60	0.03	−0.10	0.14	0.79 ± 0.60	22.52
error		1.04	0.97	0.32	0.24	0.28	0.93 ± 0.55	0

relaxation, which is captured to a great degree by the GF2 (and also GW) closures.

To further understand the error, we compare the binding energies calculated for the lowest excitation (shown in parentheses for each method). The binding energy is defined as the difference between quasiparticle gap and the lowest optical energy gap. Here, we use EOM-CCSD as our reference. We list absolute binding energy from EOM-CCSD, the error of the other method against EOM-CCSD. We find that GW-BSE and GF2-BSE agree well with the EOM-CCSD approach, while CIS/TDHF deviate significantly (except for LiF). While the overall comparison of all methods with EOM-CCSD for LiF yields rather poor results, the GF2-BSE approach seems to be systematically more accurate than CIS, TDHF, EOM-CC2, and CIS(D) for all excitations energies. The source of deviation from the EOM-CCSD approach for all methods can be traced to errors in estimating the fundamental gaps (all binding energies are very similar), where the GF2 approach provides a more accurate description leading to better agreement for the excitations energies. Note also that LiF has significant charge transfer character. In CIS/TDHF or CIS(D) method, orbital relaxations are not included, whereas in the case of GW-BSE or GF2-BSE, the orbital relaxation is incorporated in quasi-partial energy correction. We expect that GW-BSE or GF2-BSE works better for charge-transfer states. This will be further tested in future studies.

In Tables 4 and 5, we compare the GF2-BSE excited states for several additional systems. Since EOM-CCSD predicts very similar results as compared to EOM-CC(2,3), we now use EOM-CCSD as our reference. For these systems, the performance of TDHF/CIS is rather poor. Note that the ordering of the low lying excitation energies from different methods can be different. For instance, the $1B_{3g}$ state of N_2 molecule is the first excited state in EOM-CCSD, which is the fourth excited state in CIS method. We label the ordering in energy for the methods when the ordering is different from EOM-CCSD ordering. We note in passing that for the GF2 calculations, we do not use symmetry to order the states but instead, average the results over 10 independent runs. Each stochastic run may results in different ordering of the states and the results presented in this work simply average over these fluctuations. Thus, the symmetry of the states within sGF2 is difficult to determine and perhaps required better statistical averaging.

In Tables 6 and 7, we examine the performance of the GF2-BSE approach for different system and basis set sizes. We have used C_nH_{2n+2} and HF as our test systems. Note that the performance of GF2-BSE does not seems to be dependent strongly on the system or basis set size, and as before, the GW-BSE and GF2-BSE perform much better than TDHF/CIS. For these choices of molecules, CIS(D) and EOM-CC2 perform very well, compared to EOM-CCSD, as there is no strong charge transfer characters in these systems.

https://doi.org/10.1021/acs.jctc.2c00057
J. Chem. Theory Comput. XXXX, XXX, XXX−XXX

V. CONCLUSIONS

We have developed a time-dependent second-order Green's function theory to describe the response of a many-body molecular system to an external driving force. In principle, the framework can be combined with the stochastic resolution of identity to reduce the scaling to $O(N^3)$ in both the weak and strong driving fields. In the present work, we have further introduced a linear-response approach for weak driving fields, which allowed us to recast the equation of motion for the time-dependent second-order Green's function into a frequency domain Casida-like equation (GF2-BSE).

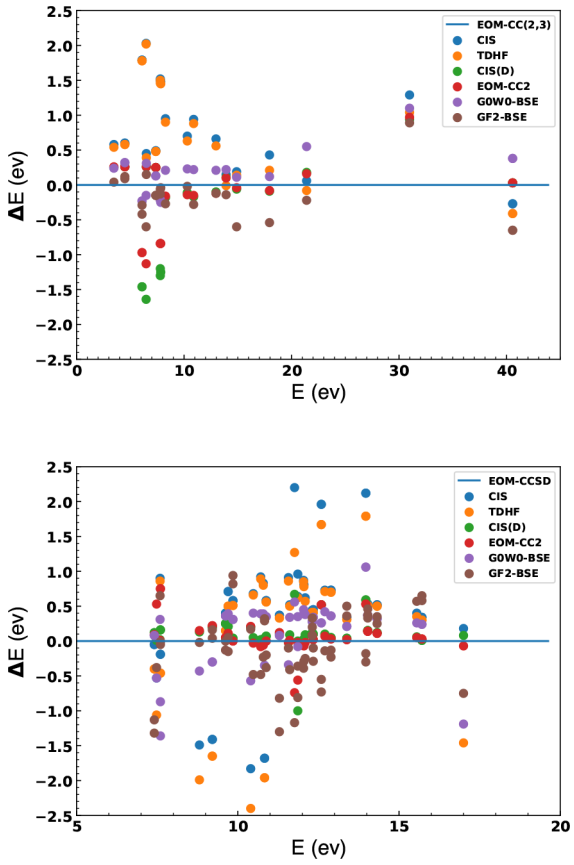

Figure 1. Error of excited-state energies listed in the above tables versus the EOM-CCSD or EOM-CC(2,3) results.

We find that the approach provides more accurate vertical excitation energies, compared to the CIS and TDHF, and is competitive with CIS(D) for a broad class of molecular systems, particularly for charge transfer excitations. Moreover, the GF2-BSE approach provides more accurate binding energies compared to the other methods, suggesting that the main source of error in the GF2-BSE approach results from underestimation/overestimation of the fundamental gaps, implying that the approach provides a reasonably accurate framework to describe electron−hole correlation, screening, and exchange in molecular systems. To better illustrate these conclusions, in Figure 1, we plot the excited-state energies listed in the aforementioned tables versus the EOM-CCSD or EOM-CC(2,3) results. Note that CIS(D), GF2-BSE, and GW-BSE results are in much better agreement with the EOM-CCSD results, compared to CIS/TDHF (the latter is not shown, but provides similar results to CIS). Overall, GF2-BSE method performs much better than CIS/TDHF, and for the lower excited-state energies, it provides similar results in comparison to CIS(D) and GW-BSE.

Given the facile route to construct a low-scaling sGF2 approach to neutral excitations, we believe GF2-BSE should be one of the methods of choice for describing binding energies in molecules. In addition, with corrected fundamental gaps, the approach should also be competitive with the most sophisticated approaches for calculating the location of low-lying excited states as well. Future work will be devoted to a full sGF2-BSE implementation as well as the reporting of a complete benchmark set of results for a wide range of molecular systems.

VI. DATA AVAILABLITY

The data that support the findings of this study are available from the corresponding author upon reasonable request.

APPENDIX A. EVALUATION OF $\tilde{\Sigma}^{\mathrm{ad}}(t)$ AND $\delta\tilde{W}^{R}_{imjn}(\omega)$

In this Appendix, we provide more details concerning the evaluation of $\tilde{\Sigma}^{\mathrm{ad}}(t)$ and $\delta\tilde{W}^{\mathrm{R}}_{imjn}(\omega)$ appearing in Sections II and III of the main text. The retarded self-energy in the second-order Born approximation is given by eq 11. We have also defined $\delta W^{R}_{imjn}(t_1, t_2)$ and $\delta W^{>}_{imjn}(t_1, t_2)$ in eq 12. The retarded self-energy given in eq 11 has two terms when Langreth rules are employed. The first term can be evaluated at $t = 0$ to give

$$\begin{aligned}\tilde{\Sigma}^{\mathrm{ad1}}_{ij}(t=0,\omega) &= i\sum_{mn}\int\frac{\mathrm{d}\omega_1}{2\pi}\delta\tilde{W}^{R}_{imjn}(\omega-\omega_1)G^{<}_{mn}(\omega_1)\\ &= i\sum_{mn}\int\frac{\mathrm{d}\omega_1}{2\pi}\delta\tilde{W}^{R}_{imjn}(\omega-\omega_1)2\pi i\delta(\omega_1-E_m)f(\omega)\delta_{mn}\\ &= i\sum_{mn}\delta\tilde{W}^{R}_{imjn}(\omega-E_m)if(E_m)\delta_{mn}\end{aligned} \tag{A1}$$

To obtain $\tilde{\Sigma}^{\mathrm{ad1}}_{ij}(t, \omega)$ at any time, we replace $if(E_m)\delta_{mn}$ by $G^{<}(t, \tau = 0)$, such that

$$\tilde{\Sigma}^{\mathrm{ad1}}_{ij}(t,\omega) = i\sum_{mn}\delta\tilde{W}^{R}_{imjn}(\omega-E_m)G^{<}_{mn}(t,\tau=0) \tag{A2}$$

Similar steps can be taken for the second term in eq 11,

$$\begin{aligned}\tilde{\Sigma}^{\mathrm{ad2}}_{ij}(t=0,\omega) &= i\sum_{mn}\int\frac{\mathrm{d}\omega_1}{2\pi}\tilde{G}^{R}_{mn}(\omega-\omega_1)\delta\tilde{W}^{>}_{imjn}(\omega_1)\\ &= i\sum_{mn}\int_{-\infty}^{\infty}\frac{\mathrm{d}\omega_1}{2\pi}\frac{1}{\omega-\omega_1-E_m+i\eta}\\ &\quad\times\delta_{mn}2i\mathrm{Im}\,\delta\tilde{W}^{R}_{imjn}(\omega_1)\Theta(\omega_1)\end{aligned} \tag{A3}$$

In the above, we have used the known relation for the noninteracting GF, $\tilde{G}^{<}_{mn}(t=0,\omega) = i2\pi\delta(\omega-E_n)f(\omega)\delta_{mn}$, as well as the fluctuation−dissipation theorem at zero temperature:

$$\delta\tilde{W}^{>}_{imjn}(\omega_1) = 2i\mathrm{Im}\,\delta\tilde{W}^{R}_{imjn}(\omega_1)\Theta(\omega_1) \tag{A4}$$

where $\Theta(\omega_1)$ is a step function. Taking the real part of the above equation and using the Kramers−Kronig relationship, we obtain

https://doi.org/10.1021/acs.jctc.2c00057
J. Chem. Theory Comput. XXXX, XXX, XXX−XXX

$$\tilde{\Sigma}^{\mathrm{ad2}}_{ij}(t=0,\omega) = \Re\sum_{mn}\delta\tilde{W}^{R}_{imjn}(\omega-E_m)\Theta(\omega-E_m)\delta_{mn} \approx \frac{1}{2}\Re\sum_{mn}\delta\tilde{W}^{R}_{imjn}(0)\delta_{mn} \tag{A5}$$

Similarly, we can evaluate $\delta\tilde{W}^{R}_{im,jn}(\omega)$ appearing in the above equations. We first Fourier transform eq 12 to obtain

$$\delta\tilde{W}^{R}_{imjn}(\omega) = -i\sum_{klpq}\int\frac{\mathrm{d}\omega_1}{2\pi}(\tilde{G}^{<}_{kl}(\omega)\tilde{G}^{A}_{qp}(\omega-\omega_1) + \tilde{G}^{R}_{kl}(\omega)\tilde{G}^{<}_{qp}(\omega-\omega_1))v_{impk}(2v_{jnql}-v_{jlqn}) \tag{A6}$$

Using the noninteracting Green's functions, we arrive at the working expression for $\delta\tilde{W}^{R}_{imjn}(\omega)$ in eq 22.

APPENDIX B. LINEAR RESPONSE REGIME

The derivation in this section closely follows the one for TDDFT.[10] We first define

$$\mathcal{F} = F + \tilde{\Sigma}^{ad} \tag{B1}$$

The equation of motion for the density operator in the molecular basis can be written as

$$i\partial_t\rho = \mathcal{F}\rho - \rho\mathcal{F}^{\dagger} \tag{B2}$$

The unperturbed density matrix can be written in a matrix form:

$$\rho_0 = \begin{pmatrix} I_{oo} & 0 \\ 0 & 0 \end{pmatrix} \tag{B3}$$

Here, o and v indicate occupied and virtual subspace. The time-dependent perturbation is assumed to take the following form:

$$\delta\mathcal{F}(t) = \begin{pmatrix} 0 & \delta\mathcal{F}^{(\omega)}_{ov}\mathrm{e}^{i\omega t} \\ \delta\mathcal{F}^{(\omega)}_{vo}\mathrm{e}^{-i\omega t} & 0 \end{pmatrix} + \begin{pmatrix} 0 & \delta\mathcal{F}^{(-\omega)}_{ov}\mathrm{e}^{-i\omega t} \\ \delta\mathcal{F}^{(-\omega)}_{vo}\mathrm{e}^{i\omega t} & 0 \end{pmatrix} \tag{B4}$$

Similarly, the perturbed density is assumed to be

$$\delta\rho(t) = \begin{pmatrix} 0 & \delta\rho^{(\omega)}_{ov}\mathrm{e}^{i\omega t} \\ \delta\rho^{(\omega)}_{vo}\mathrm{e}^{-i\omega t} & 0 \end{pmatrix} + \begin{pmatrix} 0 & \delta\rho^{(-\omega)}_{ov}\mathrm{e}^{-i\omega t} \\ \delta\rho^{(-\omega)}_{vo}\mathrm{e}^{i\omega t} & 0 \end{pmatrix} \tag{B5}$$

The equation of motion for the perturbed density then can be obtained:

$$i\partial_t\delta\rho_{vo}(t) = \delta\mathcal{F}_{vo} + \mathcal{F}_{vv}\delta\rho_{vo} - \delta\rho_{vo}F_{oo} \tag{B6}$$

Collecting $\mathrm{e}^{-i\omega t}$ and $\mathrm{e}^{-i\omega t}$ terms separately, we arrive at

$$(\omega-\omega_a+\omega_i)\delta\rho^{(\omega)}_{ai} = \delta\mathcal{F}^{(\omega)}_{ai} \tag{B7}$$

$$(-\omega-\omega_a+\omega_i)\delta\rho^{(-\omega)}_{ai} = \delta\mathcal{F}^{(-\omega)}_{ai} \tag{B8}$$

The right-hand side of the above equations can be further evaluated in the linear regime:

$$\delta\mathcal{F}^{(\omega)}_{ai} = \sum_{bj}\frac{\partial\mathcal{F}_{ai}}{\partial\rho_{bj}}\delta\rho^{(\omega)}_{bj} + \frac{\partial\mathcal{F}_{ai}}{\partial\rho_{jb}}\delta\rho^{(-\omega)}_{jb} = \sum_{bj}(A_{aibj}-(\omega_a-\omega_i)\delta_{ab}\delta_{ij})\delta\rho^{(\omega)}_{bj} + B_{aibj}\delta\rho^{(-\omega)}_{jb} \tag{B9}$$

Similarly, one gets

$$\delta\mathcal{F}^{(-\omega)}_{ai} = \sum_{bj}\frac{\partial\mathcal{F}_{ai}}{\partial\rho_{bj}}\delta\rho^{(-\omega)}_{bj} + \frac{\partial\mathcal{F}_{ai}}{\partial\rho_{jb}}\delta\rho^{(\omega)}_{jb} = \sum_{bj}(A_{aibj}-(\omega_a-\omega_i)\delta_{ab}\delta_{ij})\delta\rho^{(-\omega)}_{bj} + B_{aibj}\delta\rho^{(\omega)}_{jb} \tag{B10}$$

Here, A_{aibj} and B_{aibj} are defined in the main text. The matrix representation of the above equations is the Casida equation in the main text.

ASSOCIATED CONTENT

Supporting Information

The Supporting Information is available free of charge at https://pubs.acs.org/doi/10.1021/acs.jctc.2c00057.

Geometries of the molecules (PDF)

AUTHOR INFORMATION

Corresponding Authors

Wenjie Dou − *Department of Chemistry, School of Science, Westlake University, Hangzhou, Zhejiang 310024, China; Department of Physics, School of Science, Westlake University, Hangzhou, Zhejiang 310024, China; Institute of Natural Sciences, Westlake Institute for Advanced Study, Hangzhou, Zhejiang 310024, China;* orcid.org/0000-0001-5410-6183; Email: douwenjie@westlake.edu.cn

Joonho Lee − *Department of Chemistry, Columbia University, New York, New York 10027, United States;* orcid.org/0000-0002-9667-1081; Email: jl5653@columbia.edu

Jian Zhu − *Department of Chemistry, School of Science, Westlake University, Hangzhou, Zhejiang 310024, China; Institute of Natural Sciences, Westlake Institute for Advanced Study, Hangzhou, Zhejiang 310024, China*; Email: zhujian@westlake.edu.cn

Leopoldo Mejía − *Department of Chemistry, University of California, Berkeley, California 94720, United States; Materials Sciences Division, Lawrence Berkeley National Laboratory, Berkeley, California 94720, United States;* orcid.org/0000-0003-4534-0191; Email: leopoldo.mejia@berkeley.edu

David R. Reichman − *Department of Chemistry, Columbia University, New York, New York 10027, United States*; Email: drr2103@columbia.edu

Roi Baer − *Fritz Haber Center for Molecular Dynamics, Institute of Chemistry, The Hebrew University of Jerusalem, Jerusalem 91904, Israel;* orcid.org/0000-0001-8432-1925; Email: roi.baer@huji.ac.il

Eran Rabani − *Department of Chemistry, University of California, Berkeley, California 94720, United States; Materials Sciences Division, Lawrence Berkeley National Laboratory, Berkeley, California 94720, United States; The*

https://doi.org/10.1021/acs.jctc.2c00057
J. Chem. Theory Comput. XXXX, XXX, XXX−XXX

Raymond and Beverly Sackler Center of Computational Molecular and Materials Science, Tel Aviv University, Tel Aviv 69978, Israel; orcid.org/0000-0003-2031-3525; Email: eran.rabani@berkeley.edu

Complete contact information is available at: https://pubs.acs.org/10.1021/acs.jctc.2c00057

Notes

The authors declare no competing financial interest.

■ ACKNOWLEDGMENTS

We would like to thank Yang-Hao Chen, Daniel Neuhauser, Vojtech Vlcek for helpful discussions. R.B. gratefully acknowledges support from the U.S.−Israel Binational Science Foundation (No. BSF-201836). E.R. and D.R.R. are grateful for support by the U.S. Department of Energy, Office of Science, Office of Advanced Scientific Computing Research, Scientific Discovery through Advanced Computing (SciDAC) program, under Award No. DE-SC0022088. The stochastic methods[45,61] used in this work were provided by the Center for Computational Study of Excited State Phenomena in Energy Materials (C2SEPEM), which is funded by the U.S. Department of Energy, Office of Science, Basic Energy Sciences, Materials Sciences and Engineering Division, via contract no. DE-AC02-05CH11231, as part of the Computational Materials Sciences Program. Resources of the National Energy Research Scientific Computing Center (NERSC), a U.S. Department of Energy Office of Science User Facility operated under Contract No. DE-AC02-05CH11231 are greatly acknowledged.

■ REFERENCES

(1) McLachlan, A.; Ball, M. *Rev. Mod. Phys.* **1964**, *36*, 844.
(2) Hirata, S.; Head-Gordon, M.; Bartlett, R. J. *J. Chem. Phys.* **1999**, *111*, 10774.
(3) Runge, E.; Gross, E. K. U. *Phys. Rev. Lett.* **1984**, *52*, 997.
(4) Hirata, S.; Head-Gordon, M. *Chem. Phys. Lett.* **1999**, *314*, 291.
(5) Van Leeuwen, R. *Int. J. Mod. Phys. B* **2001**, *15*, 1969.
(6) Onida, G.; Reining, L.; Rubio, A. *Rev. Mod. Phys.* **2002**, *74*, 601.
(7) Hessler, P.; Maitra, N. T.; Burke, K. *J. Chem. Phys.* **2002**, *117*, 72.
(8) Marques, M.; Gross, E. *Annu. Rev. Phys. Chem.* **2004**, *55*, 427.
(9) Jacquemin, D.; Wathelet, V.; Perpete, E. A.; Adamo, C. *J. Chem. Theory Comput.* **2009**, *5*, 2420.
(10) Casida, M. E. *J. Mol. Struct.* **2009**, *914*, 3.
(11) Albrecht, S.; Reining, L.; Del Sole, R.; Onida, G. *Phys. Rev. Lett.* **1998**, *80*, 4510.
(12) Benedict, L. X.; Shirley, E. L.; Bohn, R. B. *Phys. Rev. Lett.* **1998**, *80*, 4514.
(13) Rohlfing, M.; Louie, S. G. *Phys. Rev. B* **2000**, *62*, 4927.
(14) Benedict, L. X.; Puzder, A.; Williamson, A. J.; Grossman, J. C.; Galli, G.; Klepeis, J. E.; Raty, J.-Y.; Pankratov, O. *Phys. Rev. B* **2003**, *68*, 085310.
(15) Spataru, C. D.; Ismail-Beigi, S.; Benedict, L. X.; Louie, S. G. *Phys. Rev. Lett.* **2004**, *92*, 077402.
(16) Tiago, M. L.; Chelikowsky, J. R. *Phys. Rev. B* **2006**, *73*, 205334.
(17) Sai, N.; Tiago, M. L.; Chelikowsky, J. R.; Reboredo, F. A. *Phys. Rev. B* **2008**, *77*, 161306.
(18) Rocca, D.; Ping, Y.; Gebauer, R.; Galli, G. *Phys. Rev. B* **2012**, *85*, 045116.
(19) Fuchs, F.; Rödl, C.; Schleife, A.; Bechstedt, F. *Phys. Rev. B* **2008**, *78*, 085103.
(20) Ramos, L.; Paier, J.; Kresse, G.; Bechstedt, F. *Phys. Rev. B* **2008**, *78*, 195423.
(21) Palummo, M.; Hogan, C.; Sottile, F.; Bagalá, P.; Rubio, A. *J. Chem. Phys.* **2009**, *131*, 084102.
(22) Schimka, L.; Harl, J.; Stroppa, A.; Grüneis, A.; Marsman, M.; Mittendorfer, F.; Kresse, G. *Nat. Mater.* **2010**, *9*, 741.
(23) Rocca, D.; Lu, D.; Galli, G. *J. Chem. Phys.* **2010**, *133*, 164109.
(24) Blase, X.; Attaccalite, C.; Olevano, V. *Phys. Rev. B* **2011**, *83*, 115103.
(25) Faber, C.; Duchemin, I.; Deutsch, T.; Blase, X. *Phys. Rev. B* **2012**, *86*, 155315.
(26) Faber, C.; Boulanger, P.; Attaccalite, C.; Duchemin, I.; Blase, X. *Philos. Trans. R. Soc. A: Math., Phys. Eng. Sci.* **2014**, *372*, 20130271.
(27) Shishkin, M.; Kresse, G. *Phys. Rev. B* **2007**, *75*, 235102.
(28) Caruso, F.; Rinke, P.; Ren, X.; Rubio, A.; Scheffler, M. *Phys. Rev. B* **2013**, *88*, 075105.
(29) Neuhauser, D.; Gao, Y.; Arntsen, C.; Karshenas, C.; Rabani, E.; Baer, R. *Phys. Rev. Lett.* **2014**, *113*, 076402.
(30) Rabani, E.; Baer, R.; Neuhauser, D. *Phys. Rev. B* **2015**, *91*, 235302.
(31) Nguyen, H.-V.; Pham, T. A.; Rocca, D.; Galli, G. *Phys. Rev. B* **2012**, *85*, 081101.
(32) Deslippe, J.; Samsonidze, G.; Strubbe, D. A.; Jain, M.; Cohen, M. L.; Louie, S. G. *Comput. Phys. Commun.* **2012**, *183*, 1269.
(33) Foerster, D.; Koval, P.; Sánchez-Portal, D. *J. Chem. Phys.* **2011**, *135*, 074105.
(34) Gonze, X.; Amadon, B.; Anglade, P.-M.; Beuken, J.-M.; Bottin, F.; Boulanger, P.; Bruneval, F.; Caliste, D.; Caracas, R.; Côté, M.; Deutsch, T.; Genovese, L.; Ghosez, P.; Giantomassi, M.; Goedecker, S.; Hamann, D.; Hermet, P.; Jollet, F.; Jomard, G.; Leroux, S.; Mancini, M.; Mazevet, S.; Oliveira, M.; Onida, G.; Pouillon, Y.; Rangel, T.; Rignanese, G.-M.; Sangalli, D.; Shaltaf, R.; Torrent, M.; Verstraete, M.; Zerah, G.; Zwanziger, J. *Comput. Phys. Commun.* **2009**, *180*, 2582.
(35) Phillips, J. J.; Zgid, D. *J. Chem. Phys.* **2014**, *140*, 241101.
(36) Pavošević, F.; Peng, C.; Ortiz, J.; Valeev, E. F. *J. Chem. Phys.* **2017**, *147*, 121101.
(37) Ohnishi, Y.-y.; Ten-no, S. *J. Comput. Chem.* **2016**, *37*, 2447.
(38) Stefanucci, G.; van Leeuwen, R. *Nonequilibrium Many-Body Theory of Quantum Systems: A Modern Introduction*; Cambridge University Press, 2013.
(39) Kananenka, A. A.; Phillips, J. J.; Zgid, D. *J. Chem. Theory Comput.* **2016**, *12*, 564.
(40) Cederbaum, L. *J. Phys. B* **1975**, *8*, 290.
(41) Holleboom, L.; Snijders, J. *J. Chem. Phys.* **1990**, *93*, 5826.
(42) Dahlen, N. E.; van Leeuwen, R.; von Barth, U. *Int. J. Quantum Chem.* **2005**, *101*, 512.
(43) Takeshita, T. Y.; de Jong, W. A.; Neuhauser, D.; Baer, R.; Rabani, E. *J. Chem. Theory Comput.* **2017**, *13*, 4605.
(44) Takeshita, T. Y.; Dou, W.; Smith, D. G.; de Jong, W. A.; Baer, R.; Neuhauser, D.; Rabani, E. *J. Chem. Phys.* **2019**, *151*, 044114.
(45) Dou, W.; Takeshita, T. Y.; Chen, M.; Baer, R.; Neuhauser, D.; Rabani, E. *J. Chem. Theory Comput.* **2019**, *15*, 6703.
(46) Whitten, J. L. *J. Chem. Phys.* **1973**, *58*, 4496.
(47) Dunlap, B. I. Fitting the Coulomb potential variationally in Xα molecular calculations. *J. Chem. Phys.* **1983**, *78*, 3140.
(48) Dunlap, B. I.; Connolly, J. W. D.; Sabin, J. R. *J. Chem. Phys.* **1979**, *71*, 3396.
(49) Vahtras, O.; Almlöf, J.; Feyereisen, M. W. *Chem. Phys. Lett.* **1993**, *213*, 514.
(50) Feyereisen, M.; Fitzgerald, G.; Komornicki, A. *Chem. Phys. Lett.* **1993**, *208*, 359.
(51) Vlček, V.; Li, W.; Baer, R.; Rabani, E.; Neuhauser, D. *Phys. Rev. B* **2018**, *98*, 075107.
(52) Baer, R.; Neuhauser, D.; Rabani, E. *Phys. Rev. Lett.* **2013**, *111*, 106402.
(53) Neuhauser, D.; Baer, R.; Rabani, E. *J. Chem. Phys.* **2014**, *141*, 041102.
(54) Cytter, Y.; Neuhauser, D.; Baer, R. *J. Chem. Theory Comput.* **2014**, *10*, 4317.
(55) Chen, M.; Baer, R.; Neuhauser, D.; Rabani, E. *J. Chem. Phys.* **2019**, *150*, 034106.
(56) Neuhauser, D.; Rabani, E.; Baer, R. *J. Chem. Theory Comput.* **2013**, *9*, 24.

(57) Ge, Q.; Gao, Y.; Baer, R.; Rabani, E.; Neuhauser, D. *J. Phys. Chem. Lett.* **2014**, *5*, 185.
(58) Schäfer, T.; Ramberger, B.; Kresse, G. *J. Chem. Phys.* **2018**, *148*, 064103.
(59) Neuhauser, D.; Rabani, E.; Baer, R. *J. Chem. Phys. Lett.* **2013**, *4*, 1172.
(60) Lee, J.; Reichman, D. R. *J. Chem. Phys.* **2020**, *153*, 044131.
(61) Dou, W.; Chen, M.; Takeshita, T. Y.; Baer, R.; Neuhauser, D.; Rabani, E. *J. Chem. Phys.* **2020**, *153*, 074113.
(62) Christiansen, O.; Koch, H.; Jørgensen, P. *Chem. Phys. Lett.* **1995**, *243*, 409.
(63) Attaccalite, C.; Grüning, M.; Marini, A. *Phys. Rev. B* **2011**, *84*, 245110.
(64) Spataru, C. D.; Benedict, L. X.; Louie, S. G. *Phys. Rev. B* **2004**, *69*, 205204.

https://doi.org/10.1021/acs.jctc.2c00057
J. Chem. Theory Comput. XXXX, XXX, XXX−XXX